1   **Drought Legacies Mediated by Trait Tradeoffs in Soil Microbiomes**

2

3   Bin Wang 1, Steven D. Allison 1,2

4   1 Department of Ecology and Evolutionary Biology, University of California, Irvine, CA

5   2 Department of Earth System Science, University of California, Irvine, CA

6

7

8

9

10

11

12

13

14

15

16

17

18

19

20

21

22

23

24 **Abstract:** Soil microbiomes play a key role in driving biogeochemical cycles of the Earth system.

25 As drought frequency and intensity increase due to climate change, soil microbes and the processes

26 they control will be impacted. Even after a drought ends, microbiomes and other systems take time

27 to recover and may display a "memory" of previous climate conditions. Still, the mechanisms

28 involved in these legacy effects remain unclear, making it difficult to predict climate and

29 biogeochemical rates in the future. Here, we used a trait-based microbiome model to analyze

30 mechanisms underlying drought legacy effects on litter decomposition. We represented cellular

31 tradeoffs between osmolytes required for drought tolerance and investment in enzymes involved

32 in litter decomposition. Simulations were run under varying levels of drought severity and

33 dispersal. When dispersal was restricted, we found persistent drought legacies following severe

34 drought and transient legacies following moderate drought. With dispersal, there were no legacy

35 effects on litter decomposition. Greater movement along the tradeoff between enzyme investment

36 and osmolyte production resulted in stronger legacy effects. We organized these legacy outcomes

37 according to the YAS framework defined by tradeoffs between Y (Yield), A (Acquisition), and S

38 (Stress tolerance), three primary life history strategies of microorganisms. Factors that change the

39 trajectory of a community in YAS space may alter the legacy outcome following drought. This

40 trait-based mechanistic insight into drought legacies offers promise for more accurately predicting

41 soil microbiome resilience and functioning. Our study illustrates an emerging approach for

42 representing trait tradeoffs in microbiome and vegetation communities that dictate ecosystem

43 responses to drought and other environmental perturbations.

44

1 Introduction

Drought of increasing severity and frequency both regionally and worldwide is an important environmental change affecting the Earth system (e.g., **Borsa et al. 2014; Berdugo et al. 2020**). The soil microbiome is a key driver of element cycling (e.g., **Falkowski et al. 2008**), so microbial responses are integral for evaluating drought impacts on ecosystem biogeochemistry. Still, these responses are omitted or implicitly treated in global assessments of drought-biosphere interactions (e.g., **Green et al. 2019**).

Over a-half century of research has uncovered a myriad of physio-chemical, physiological, and ecological mechanisms underlying microbial functional responses to drought disturbance in soil environments (e.g., **Birch 1958; Schimel 2007; Manzoni et al. 2012**). However, multiple studies have suggested that drought may have lasting effects on the soil microbiome and its functioning, even after drought conditions have ended (e.g., **Evans and Wallenstein 2012**; **Meisner et al. 2015**; **Hawkes et al. 2017; Martiny et al. 2017; Hinojosa et al. 2019**). This phenomenon, here termed drought legacy, has also been observed in forests and other biomes (e.g., **Cuddington 2011; Anderegg et al. 2015; Conradi et al. 2020**). Still, the mechanistic basis for microbial drought legacies remains unclear. Such a lack of mechanistic insights hinders the ability to predict drought impacts on ecosystem processes.

Legacies likely originate from microbiome changes that persist after a drought disturbance. Microbiomes are complex adaptive systems, with their functioning emerging from both individual variation and within-community interactions. Past lab- and field-based studies explained soil microbial drought legacies by depicting compositional differences in terms of microbial functional groups with different life-history strategies. Notably, **Hawkes and Keitt (2015)** proposed a mechanism of community shift in relative abundance of moisture generalists vs. specialists, where

68 generalists are functionally more stable than specialists with variations in moisture. This idea was

69 proposed to explain a lack of change in moisture response across sites in Texas, USA, because of

70 observed dominance by generalist taxa resulting from high variability in historical rainfall

71 (**Hawkes et al. 2017; Waring and Hawkes 2018**). Similarly, **Evans and Wallenstein** (**2014**)

72 argued soils with relatively stable moisture history had more moisture-sensitive taxa and hence

73 larger changes in biomass and composition following drought (**Evans and Wallenstein 2012**).

74   Conceptual frameworks of microbial legacies based on functional groups can help simplify

75 complex microbiomes but may obscure important physiological details. For instance, microbial

76 cells can re-direct resource allocation from exoenzyme production to osmolytes that confer

77 desiccation resistance (e.g., **Schimel 2007**), an intra-cellular metabolic strategy that displays large

78 inter-cellular variability (e.g., **Manzoni et al. 2012**). Without representing these physiological

79 processes, models may have difficulty predicting microbial community responses to drought

80 disturbance and the consequences for functioning. Addressing this challenge could help reconcile

81 studies that report drought legacies of varying magnitudes with differing time frames, including

82 those that observed no legacy (e.g., **Rousk et al. 2013; Fuchslueger et al. 2016**). A similar lack

83 of mechanistic understanding also applies to warming-induced legacies in microbiome functioning

84 (e.g., **Karhu et al. 2014**). Linking individual-level physiological variation to community-level

85 shifts could help fill this gap in knowledge of microbial functioning with environmental change.

86   Trait-based approaches for dealing with ecological complexity can bridge the gap between

87 community dynamics and physiological variation that may underpin drought legacies in

88 microbiomes. Such approaches have been established previously in plant communities (e.g.,

89 **McGill et al. 2006**), and more recently, **Malik et al. (2020)** proposed a trait-based framework—

90 Y-A-S (Yield-Acquisition-Stress)—that emphasizes tradeoffs among three primary life history

91   strategies of microorganisms. On the empirical side, a manipulative experiment in a grassland

92   ecosystem in Southern California attributed a drought legacy in litter decomposition to changes in

93   bacterial composition and associated carbohydrate degradation traits (**Martiny et al. 2017**). This

94   study illustrates the potential to establish trait-based linkages between microbial physiology and

95   community shifts underlying legacies.

96   Based on the Y-A-S framework, drought disturbance should cause cellular physiology and

97   microbial composition to shift toward drought tolerance at the expense of other traits, such as

98   investment in exoenzymes. Persistence of this functional shift could result in a drought legacy that

99   affects organic matter decomposition. With this reasoning, factors that shift microbiomes along

100   the tradeoff between enzyme investment and stress tolerance could alter the magnitude and

101   duration of drought legacies. For instance, the intensity of drought, which directly modulates

102   intracellular metabolic allocation to enzymes versus osmolytes (e.g., **Csonka 1989; Schimel 2007**),

103   may determine movement along the tradeoff and hence affect the legacy magnitude. In addition,

104   microbial dispersal (e.g., **Fukami 2015; Vila et al. 2019**) may alter drought legacies through

105   effects on community composition and dynamics that regulate drought-tolerance tradeoffs

106   (**Hawkes et al. 2017**). Therefore, we hypothesize that trait-based tradeoffs between drought

107   tolerance and enzyme investment govern drought legacies in soil microbiomes.

108   Theory-driven, trait-based models are well positioned to complement lab- and field-based

109   studies and test the mechanisms underpinning soil microbiome drought legacies. Individual-based

110   models in particular offer the ability to bridge scales from individual cells through communities to

111   ecosystems by explicitly simulating intra-cellular metabolic processes, ecological dynamics of

112   microbial communities, and emergent functioning (**Allison 2012**). Such an approach can overcome

113   some of the limitations of aggregated models that treat microbes as a single biomass pool or a few

114   discrete functional groups [see a review by **Wieder et al. (2015**)]. In addition, trait- and individual-

115   based models are appropriate for testing the null hypothesis that representing legacies would have

116   little impact on biogeochemical model predictions (**Rousk et al. 2013**).

117   The goal of our study was to analyze the trait-based, tradeoff-mediated mechanisms

118   underpinning drought legacies in soil microbiomes. Our approach applied a modelling framework

119   for soil microbial systems—DEMENTpy—that represents tradeoffs among resource acquisition

120   and drought tolerance at the physiological level along with emergent processes at the community

121   level. This individual- and trait-based model represents physiological mechanisms in a spatially-

122   explicit context. Specifically, we asked the following questions: 1) How does the magnitude of

123   drought legacy vary with drought intensity for the process of litter decomposition? 2) How does

124   microbial dispersal affect the duration and magnitude of drought legacy? 3) What are the

125   underlying changes in enzyme investment and drought tolerance traits? And 4) how do these

126   changes align with the mechanisms proposed in the YAS framework? We tackled these questions

127   by applying DEMENTpy to a grassland ecosystem in Southern California. Our study exemplifies

128   how trait-based investigations into microbiome legacies can improve mechanistic understanding

129   of element cycling in response to climate change.

130

131   **2 Methods**

132   **2.1 Model description**

133   DEMENTpy (DEcomposition Model of ENzymatic Traits in Python; GitHub Repository:

134   https://github.com/bioatmosphere/DEMENTpy) is a spatially-explicit, trait- and individual-based

135   model. Starting from continuous physiological traits, DEMENTpy bridges across soil microbiome

136   scales from individual cells through communities and systems (see **Supporting Fig. 1** for model

137 structure). Its mechanistic modelling framework is built upon its predecessor DEMENT (**Allison**

138 **2012; Allison and Goulden 2017; Wang and Allison 2019**). DEMENTpy initiates a microbial

139 community composed of a large number of hypothetical taxa by randomly drawing values from

140 uniform distributions of microbial traits and assigning them to different taxa (see a list of traits in

141 **Supporting Fig. 1B** and more details in **Supporting Text**). Community dynamics are simulated

142 by explicitly modelling demographic processes of cell metabolism and growth, mortality, and

143 reproduction for each taxon population at a daily time step. Microbial taxa secrete exoenzymes

144 (constitutive and inducible) that degrade different organic compounds at rates that depend on

145 temperature and moisture. To address questions related to drought response, the current version of

146 DEMENTpy represents explicit osmolyte production (constitutive and inducible). Drought

147 tolerance of each taxon is determined by normalizing the inducible osmolyte rate of production to

148 a value from 0 to 1. This formulation establishes a mechanistic connection between osmolyte

149 production and drought tolerance (**Schimel 2007**) in contrast to the previous model version which

150 instead directly introduced a drought tolerance parameter and imposed a penalty on carbon use

151 efficiency accordingly (**Allison and Goulden 2017**).

152 DEMENTpy tracks intra-cellular metabolism of assimilated monomer carbon derived from

153 exoenzymatic degradation of substrates (**Supporting Fig. 1C**; see **Supporting Text** for substrate

154 degradation and other demographic processes). After growth respiration, assimilated carbon is

155 directed to enzyme production, osmolyte production, and associated maintenance respiration,

156 which are treated as simultaneous processes without prescribing an order. The carbon remaining

157 after constitutive and inducible metabolite production accumulates toward biomass (denoted as

158 yield). We assume that constitutive osmolyte production varies across taxa but independent of

159 water potential, reflecting microbial allocation to maintain water potential balance across the cell

7

160   wall (e.g., **Csonka 1989; Potts 1994**). By contrast, inducible production of osmolytes occurs when

161   water potential falls below a threshold. Mortality of microbial cells is simulated both

162   deterministically by accounting for mass balance and stochastically based on death probability

163   dependent on drought tolerance and water potential. More details on model structure, processes,

164   formulae, and parameters are included in the **Supporting Information.**

165   **2.2 Modelling experiments**

166   We applied DEMENTpy to a grassland ecosystem at Loma Ridge, Southern California

167   (**Allison et al. 2013**) and parameterized the model with 100 different hypothetical bacterial taxa

168   on a 100 by 100 spatial grid with decomposing grass litter containing ten different substrates (see

169   parameter values in **Supporting Table 1** and substrates in **Supporting Table 2**). DEMENTpy was

170   forced with daily weather data from the year 2011, which is designated as the ambient scenario

171   (**Supporting Fig. 2A**). In addition to this ambient scenario, we conducted simulations to examine

172   drought disturbance response and recovery in three phases (**Supporting Fig. 2**). Two drought

173   scenarios, moderate and severe, were generated by reducing the water potential during the dry

174   season by a factor of four and ten, respectively. After a community establishment phase and a

175   successive drought period, ambient conditions were re-imposed to test for legacy effects on

176   microbial communities and substrate decomposition. Simulations in "default" mode did not allow

177   for microbial dispersal; once taxa disappeared from a default simulation, they could not return. We

178   also ran simulations in "dispersal" mode to test how dispersal affects drought response and legacy

179   effects. In contrast to the default mode, dispersal mode allows extinct taxa to recolonize at the start

180   of each model year. This mode accounts for the possibility that bacterial populations survive in

181   local refugia or nearby wetter areas and then disperse on to fresh litter.

182   **2.3 Simulation protocol**

183   After establishing an initial microbial community from a randomly constructed microbial

184   pool on the spatial grid with homogeneously distributed substrates, each simulation was run for 10

185   years at a daily time step (spin-up: 3 years; drought disturbance: 3 years; recovery: 4 years)

186   (**Supporting Fig. 2**). Substrates, monomers, and enzymes were reinitialized uniformly on the

187   spatial grid at the start of each new year to have the same concentrations as the first year. At the

188   start of each year, the microbial community on the spatial grid was randomly reinitialized with the

189   same total microbial biomass. Two methods were applied to differentiate between the default and

190   dispersal modes: for the default mode, microbial community composition was determined

191   according to the biomass frequency of each taxon on the last day of the previous year (**Supporting**

192   **Fig. 2C**); in dispersal mode, the taxon frequencies were based on the cumulative biomass of each

193   taxon across the entire previous year (**Supporting Fig. 2D**). Simulations were repeated 40 times

194   for each scenario under the two modes (default and dispersal) with 40 different random number

195   generation seeds ($5 \times 40 = 200$ runs in total). This sample size was determined by a convergence

196   analysis of DEMENTpy's stochastic nature (**Supporting Fig. 3**).

197   **2.4 Data analysis**

198   Unless indicated otherwise, all analyses were conducted on the ensemble of 40 runs for

199   each of the five scenarios. Datasets extracted from these simulations included: taxon traits (enzyme

200   investment and drought tolerance); a time-series of taxon-specific allocation to enzymes (inducible

201   plus constitutive); osmolytes (inducible plus constitutive); yield and biomass in carbon; and a time-

202   series of compound-specific and total substrate concentrations. Taxon-specific allocations to

203   enzymes, osmolytes, and yield were aggregated to derive the corresponding community-level

204   allocation. Community-level traits of enzyme investment and drought tolerance were calculated

205   from biomass-weighted taxonomic traits (see the **Supporting Text** for calculation method).

206   Because the system stabilized within 3 years (**Supporting Fig. 2**), results up to year 9 (3rd year of

207   recovery from drought disturbance) are presented. In addition, 95% confidence intervals are shown

208   for most variables except for microbial community composition and community carbon allocation,
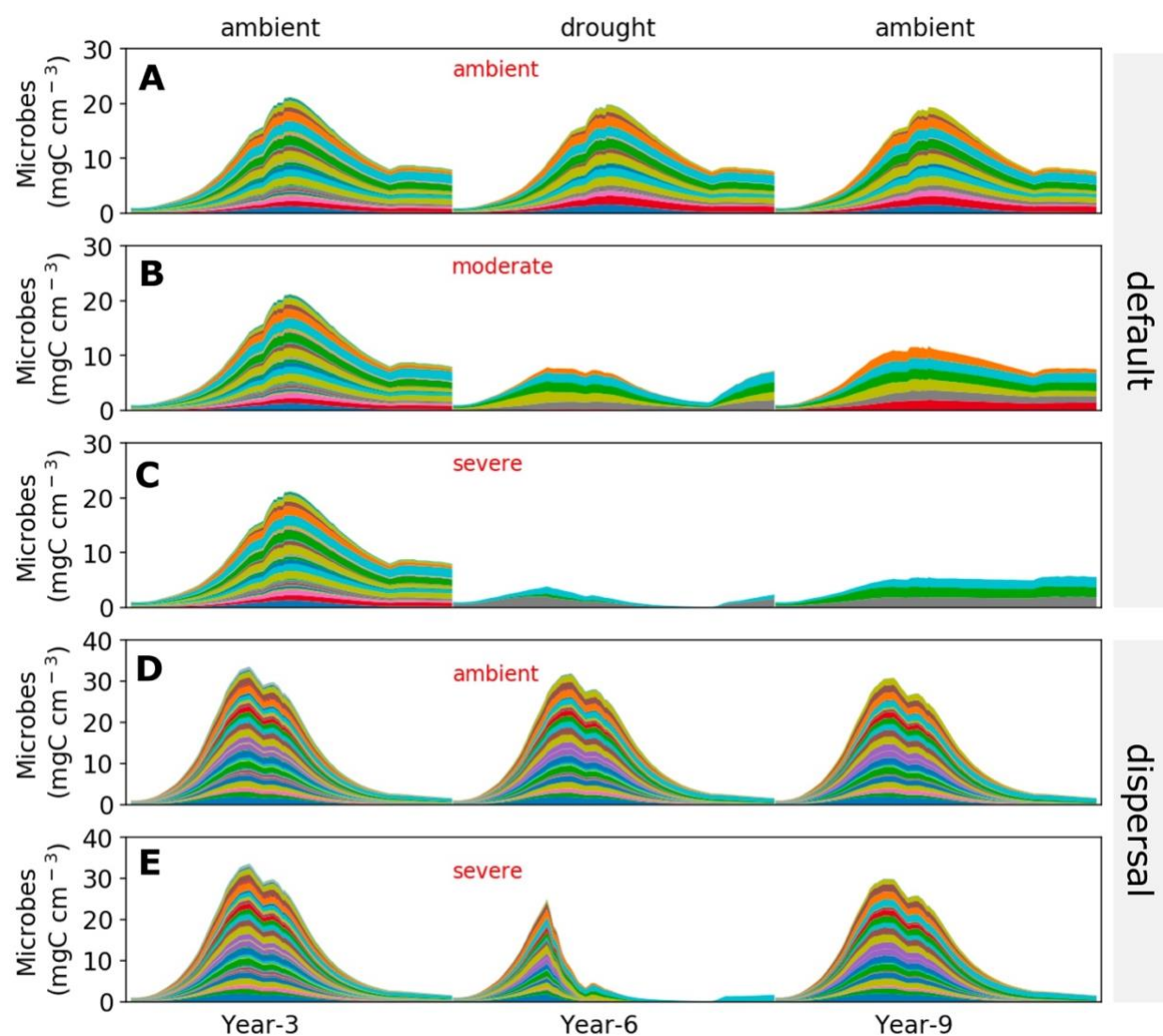
209   for which only one out of the 40 simulations are shown.

210

212   **Fig. 1. Microbial community dynamics in ambient and drought simulations with and without**

213   **dispersal.** (**A-C**) Dynamics without dispersal under ambient, moderate, and severe drought

214 scenarios, respectively. (**D, E**) Dynamics with dispersal under ambient and severe drought

215 scenarios, respectively. Colored bands represent biomass of hypothetical taxa (mg C cm$_{-3}$)

216 averaged over the 100×100 spatial grid. Data shown are only for years 3, 6 (the 3$_{rd}$ year under

217 drought), and 9 (the 3$_{rd}$ year after drought). See **Supporting Fig. 2** for the full 10-year dynamics

218 under the ambient scenario of both default and dispersal mode.

219

220 **3 Results**

221 **3.1 Microbial community dynamics under the ambient drought scenario**

222   The system became relatively stable after 2 years, with seasonal dynamics in the microbial

223 community repeating across years (**Supporting Fig. 2**). Seasonal dynamics of community

224 composition and biomass reflected a joint control by climate and substrates. Starting in the wet

225 season that was replete with substrates, the microbial community established and grew in biomass.

226 As substrates were degraded and depleted, microbial cells began to starve and die. Declining water

227 potentials after the start of the dry season induced more death. Together, these two processes

228 resulted in declining microbial biomass from a peak around 20 mg C cm$_{-3}$ (**Fig. 1A)** and drove the

229 composition toward taxa with higher drought tolerance and lower enzyme investment (**Supporting**

230 **Fig. 4A**). Hence community level enzyme investment decreased (**Fig. 2A**), and drought tolerance

231 increased across the dry season (**Fig. 2B**). Similar seasonal and inter-annual dynamics were

232 observed for the community with dispersal but with much higher biomass (peaking around 30 mg

233 C cm$_{-3}$) and taxonomic diversity (**Fig. 1D; Supporting Fig. 4B; Fig. 2C, D**).

234

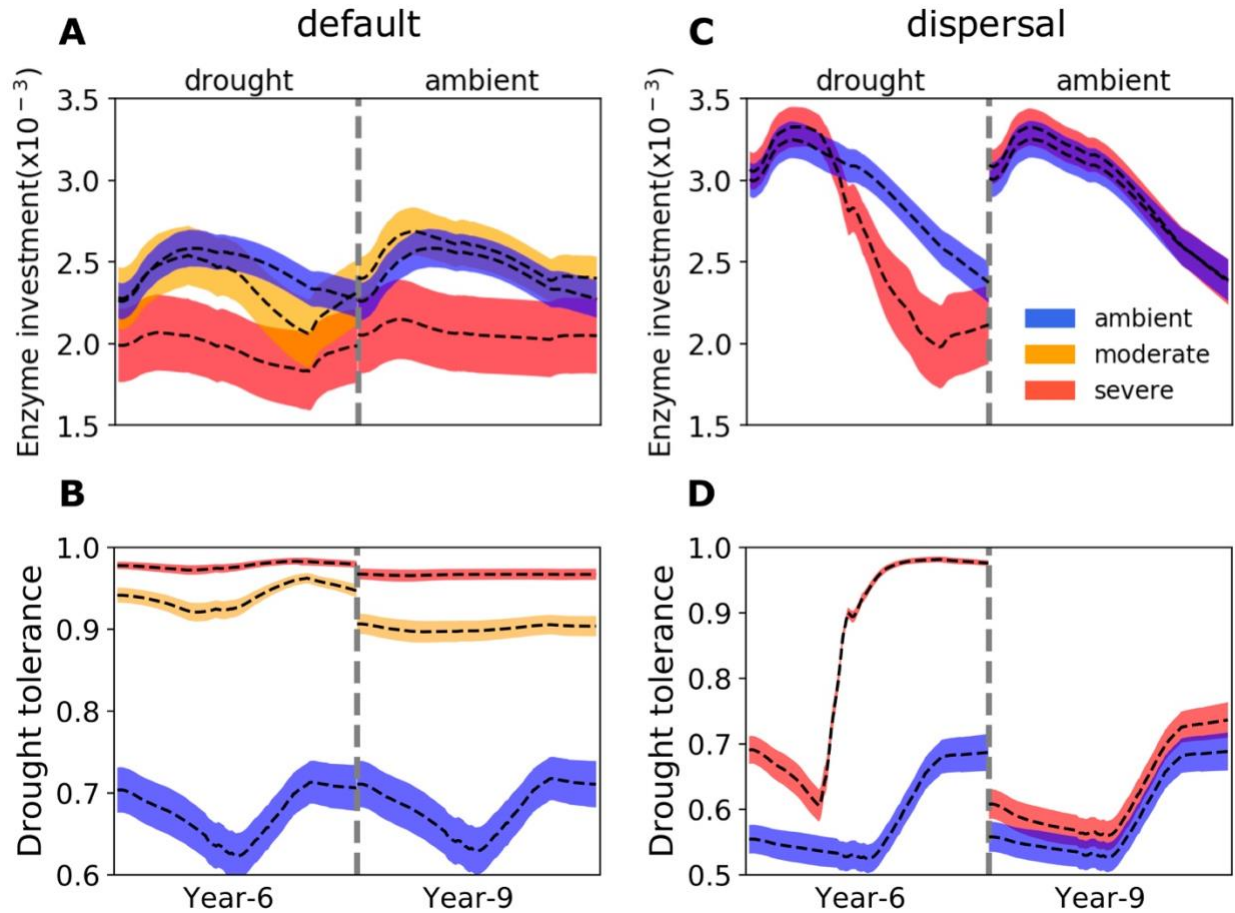**Fig. 2 Seasonal dynamics of community-level enzyme investment and drought tolerance of**

microbial communities under different drought scenarios. (**A, B**) Enzyme investment and

drought tolerance during year 6 (3rd year under drought) and year 9 (3rd year after drought) under

three drought scenarios (ambient, moderate, and severe) without dispersal, respectively. (**C, D**)

The same for communities with dispersal under two drought scenarios (ambient and severe).

Dashed lines and color bands are means and 95% confidence intervals (n=40).

241

3.2 Responses to drought disturbance of varying severity

Total biomass declined significantly under drought, with the greatest declines of nearly 50%

under the severe scenario, resulting in a peak biomass less than 10 mg C cm-3 (**Fig. 1B, C**). Severe

245   drought also had a stronger impact on microbial community composition compared to moderate

246   drought. Community taxonomic richness and functional capacity shifted dramatically after 2 years

247   of drought perturbation. Compared to the ambient scenario, drought tolerance increased

248   significantly across seasons from 0.62 up to 0.92 under the moderate scenario and up to 0.97 under

249   the severe scenario (**Fig. 2A,B**). However, the community-averaged enzyme investment only

250   declined significantly in the severe scenario across the dry season and did not change substantially

251   in the moderate scenario except late in the dry season (**Fig. 2A,B**). These trait changes reflected

252   differences in community-level carbon allocation between enzymes and osmolytes and thus yield

253   (**Fig. 3A; Supporting Fig. 5A**). Under the moderate drought scenario, the percentage of

254   assimilated carbon allocated to osmolytes ranged between 65% and 85%, compared to the ambient

255   range of 50% to 70%, whereas enzyme allocation was consistently lower (10% on average)

256   compared to the ambient scenario (20% on average). However, the resulting yield was similar,

257   ranging between 0 and 30%, although some days in the ambient scenario were higher (reaching at

258   most 40%) early in the drought season. Under the severe scenario, the allocation to osmolytes was

259   even higher and allocation to enzymes even lower, and the community yield approached zero more

260   often. These differences in community resource allocation resulted in reduced degradation of

261   substrates over the grid, with the two drought scenarios showing different rates of decomposition

262   (average of 57.39 and 85.65%, respectively; **Fig. 4A, B**).
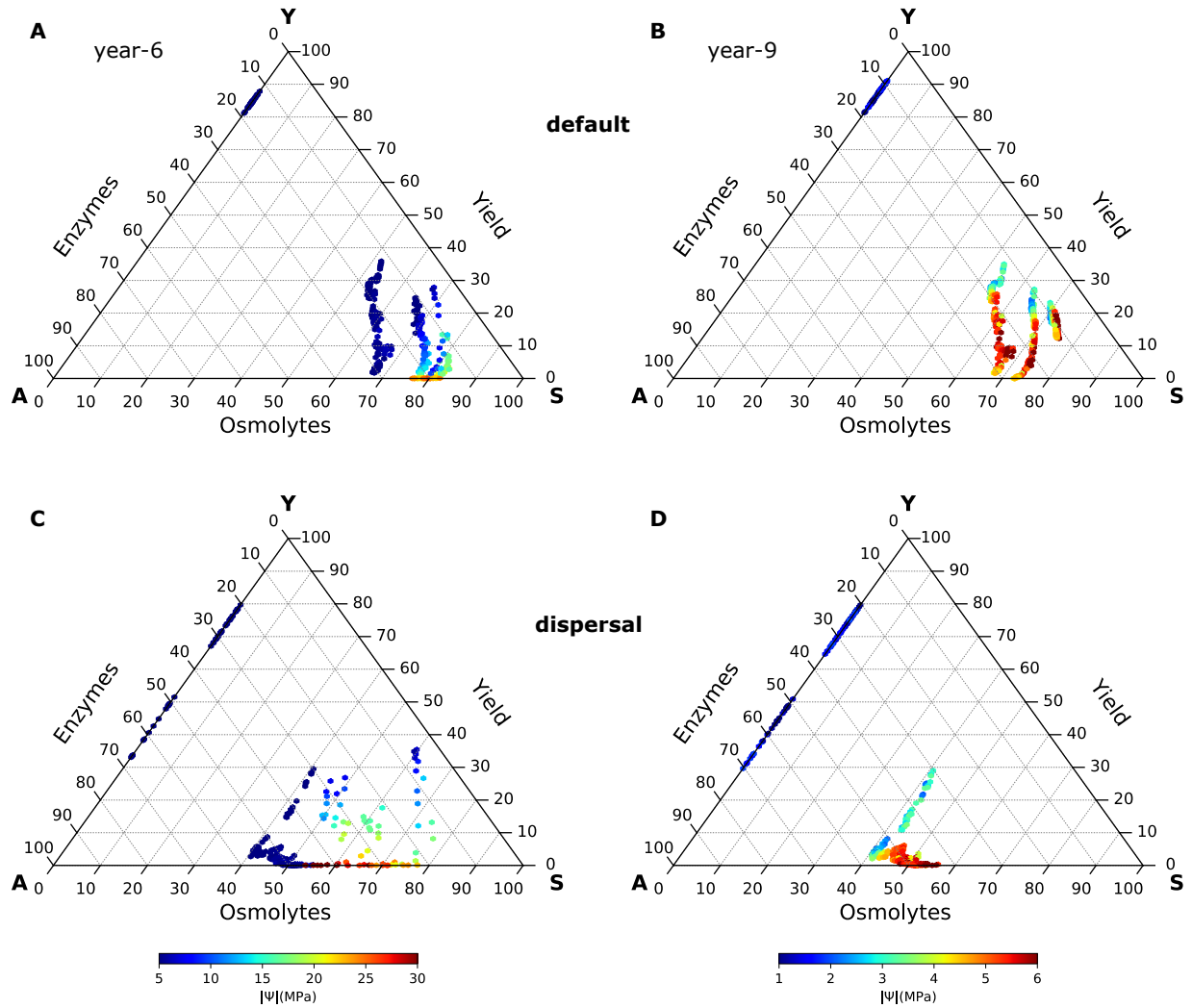
263

264

Fig. 3 Ternary plots of community-level allocation of assimilated carbon among enzymes, osmolytes, and growth yield over time under different dispersal scenarios. (A, B) Enzyme-Osmolyte-Yield tradeoff of communities during year 6 (3rd year under drought) and year 9 (3rd year after drought), respectively, of the default mode (without dispersal). (**C, D**) The same for the dispersal mode. Yield, enzymes, and osmolytes correspond to Y (Yield), A (resource Acquisition), and S (Stress) strategies labeled respectively at the triangle vertices (**Malik et al. 2020**). See **Supporting Fig. 5** for a version with points differentiated by drought scenario instead of water potential.

275   After ambient conditions were re-imposed for 2 years (i.e., by year 9), new stable microbial

276   communities assembled (**Fig. 1B, C** and **Supporting Fig. 2C**). Compared to the ambient scenario,

277   communities that re-assembled following drought had different levels of drought tolerance and

278   enzyme investment. Compared to the ambient scenario, drought tolerance remained significantly

279   higher under both the moderate drought (0.90) and severe drought (0.96) scenarios, even after

280   drought disturbance ended (**Fig. 2A**). In contrast, enzyme investment under the moderate scenario

281   became similar to the ambient community, with only the community re-assembling after severe

282   drought remaining significantly different (**Fig. 2B**). During the dry season by year 9, only the

283   severe-drought community showed a clearly lower allocation to enzymes compared to the ambient

284   community season (**Fig. 3B; Supporting Fig. 5B**). This resilience of enzyme investment in the

285   moderate-drought community meant that decomposition rates converged on ambient levels by year

286   9 (**Fig. 4A**). In contrast, substrate mass loss remained lower by 47.72% on average (**Fig. 4A**) in

287   year 9 of the severe drought scenario, although the magnitude of decline was dampened compared

288   to the antecedent drought period. Prior to year 9, the reductions in mass loss associated with

289   transient microbial communities (year 7) were significant for both drought scenarios (average

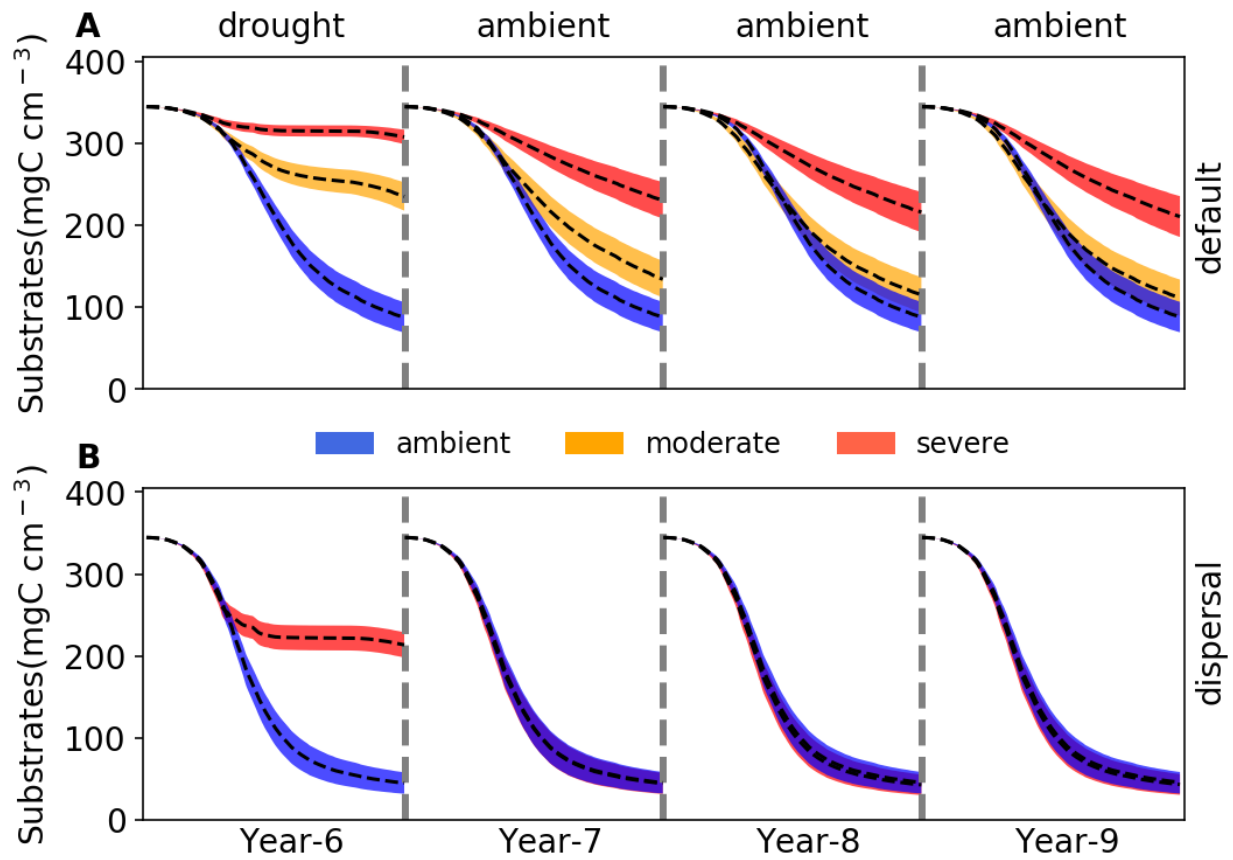290   declines of 18.00 and 55.52%, respectively).

291

292

Fig. 4 Changes in substrate concentrations during and after drought perturbation. (**A**) Total substrates on the spatial grid during years 6 to 9 under three different scenarios (ambient, moderate, and severe drought) without dispersal. (**B**) The same for simulations with dispersal under ambient and severe drought scenarios. Dashed lines and colored bands are means and 95% confidence intervals (n = 40), respectively. See **Supporting Fig. 6** for an example illustration of the underlying substrate-specific changes.

3.3 Responses to severe drought disturbance with dispersal

With dispersal of taxa from the same microbial pool at the start of each year, the direct responses to severe drought were similar to the default mode, though with differing magnitudes and seasonal patterns. With dispersal during drought disturbance, the microbial community

16

305   showed both lower total biomass and reduced taxonomic richness, particularly during the dry

306   season, though the values were higher than in the default mode (**Fig. 1E**). Community-average

307   enzyme investment and drought tolerance differed from the ambient scenario but with a different

308   seasonal pattern compared to the default mode. With the onset of the dry season, enzyme

309   investment declined sharply from a peak of 0.0033 down to 0.0020, and drought tolerance

310   increased sharply from 0.60 to 0.97, with differences from the ambient scenario increasing over

311   time (**Fig. 2C,D**). These changes reflected the community allocating more assimilated carbon to

312   produce osmolytes and less to enzymes, which resulted in zero yield when drought was most severe

313   during the dry season (**Fig. 3C; Supporting Fig. 5C**). All these changes resulted in significantly

314   lower substrate decomposition (**Fig. 4C**; an average decline of 56.29%).

315   When ambient conditions were re-imposed, recovery from drought was rapid compared to

316   the default mode. Two years after drought ended, the communities became similar in the drought

317   and ambient scenarios (**Fig. 1E**), a stark contrast to the default mode (**Fig. 1C**). This compositional

318   similarity coincided with similar community enzyme investment (**Fig. 2C**) and drought tolerance

319   (**Fig. 2D**), which resulted in the same community-level allocation of assimilated carbon among

320   enzymes (30 - 60%), osmolytes (40 - 60%), and thus yield (0 - 30%; **Fig. 3D; Supporting Fig.**

321   **5D**). These communities ultimately had almost exactly the same composition and substrate

322   decomposition rates (**Fig. 4D**). In fact, in contrast to the default mode, the transient community

323   did not even show significant differences in the 1_{st} year following drought (year 7; **Fig. 4B**). Based

324   on this clear lack of legacy effects following severe drought, we did not find it relevant to run

325   simulations of the moderate scenario with dispersal.

326

4 Discussion

By applying trait-based modelling in a mechanistically-explicit fashion, we tested the relationships between drought legacy and drought severity and dispersal in simulated litter microbiomes. Drought legacy effects on litter decomposition ranged from persistent through transient to no legacy at all and depended on drought severity and microbial dispersal (**Fig. 4**). This variation in legacy magnitude and duration showed a clear mechanistic basis—tradeoffs between enzyme production and drought tolerance, in line with the Y-A-S strategy framework. These results are relevant for understanding the resilience of microbial systems—weaker legacies correspond to higher resilience of soil microbiome functioning in response to historical drought. Our analysis of legacy mechanisms underlying microbial system resilience will help more accurately quantify carbon cycle feedbacks to drought in the Earth system.

Transient legacy under moderate drought

The severity of drought disturbance influences legacy magnitude and duration by determining the extent to which a microbial community can adapt (**Fig. 4A**). Our drought disturbance lasted long enough for communities to reach a stable state. However, our simulations focused on testing underlying mechanisms and only represent a subset of actual drought disturbances in terms of frequency, intensity, and duration. At the drought intensities we analyzed, legacies ranged from transient to persistent. Weaker disturbances might result in no legacy at all.

Drought disturbance of lower severity had a negative effect on decomposition conferred by the transient community, but eventually the legacy effect disappeared (**Fig. 4A**), a pattern that we dub "transient legacy". This transient legacy pattern matches results from a reciprocal transplant manipulation of microbial communities within a rainfall manipulation experiment at our

350   Loma Ridge field site where we observed resilience to drought in terms of litter decomposition

351   after one year (**Martiny et al. 2017**). It is noteworthy that our model-predicted transient legacy

352   arose from a community with the same functioning but different composition and biomass.

353   However, with a total biomass difference varying from 50% to essentially no difference (**Fig. 1B**),

354   the link between total biomass and functioning is likely not a major driver of the legacy pattern,

355   consistent with findings from our field experiment (**Martiny et al. 2017**) and another reciprocal

356   transplant study across a climate gradient in Southern California (**Glassman et al. 2018)**. Rather,

357   the transience of the legacy mainly resulted from convergence in community enzyme investment

358   despite lingering differences in community composition and drought tolerance (**Fig. 2A,B**). Such

359   a compositional but not functional change in an ecosystem after disturbance—which has been

360   observed before (e.g., **Fukami 2015; Ives and Carpenter 2007**)—supports the notion of

361   functional similarity in the soil microbiome (**Allison and Martiny 2008**). It is this transient legacy

362   that allows for resilience of microbial and other systems following moderate perturbation.

363   Particularly in microbial systems, functional redundancy may contribute to this resilience (e.g.,

364   **Louca et al. 2018**).

365

366   **Persistent legacy under severe drought**

367   A strong drought disturbance can push a community to reach an even higher drought

368   tolerance by sacrificing more investment in enzyme production (including a loss of relatively more

369   drought-intolerant taxa), thereby forming a community not only compositionally but also

370   functionally different (**Fig. 2A,B**). These conditions can lead to a persistent legacy (**Fig. 4B**). A

371   similar long-term legacy in soil heterotrophic respiration has also been observed in microcosm and

372   field transplant experiments (**Hawkes et al. 2017)**. This persistent legacy is consistent with the

373   idea of alternative stable states with different functioning in ecological systems (**Scheffer et al.**

374   **2001**). Disturbance-driven alternative stable states have been reported across an array of systems;

375   e.g., in gut microbiota experiencing transient osmotic perturbation (**Tropini et al. 2018**) and in

376   tropical (e.g., **Staver et al. 2011**) and boreal forests (**Herzschuh 2020**), as well as in small pond

377   systems (**Chase 2003**). Conceptually, a persistent legacy means the loss of system resilience with

378   severe disturbance (**Scheffer et al. 2001**).

379

380   **Disappearance of legacy under severe drought with dispersal**

381   Importantly, dispersal can exclude legacies in organic matter decomposition (**Fig. 4B**). By

382   re-introducing taxa from the previous year's microbial pool, we found that even with severe

383   drought, dispersal can rescue taxa from extinction and completely mitigate the effect of

384   environmental selection on the microbial community (**Fig. 1E**). By re-introducing drought

385   tolerance and enzyme investment traits (**Fig. 2C,D; Fig. 3D**), dispersal can overwhelm the drought

386   legacy in organic matter decomposition (**Fig. 4B**). This result suggests that dispersal can increase

387   microbial systems' resilience to drought disturbance (**Allison and Martiny 2008**) in stark contrast

388   to the persistent legacy induced by severe drought disturbance without dispersal (**Fig. 4B**). We

389   note that there are many dispersal factors that influence community dynamics but were not

390   represented in our model. For instance, dispersal timing (e.g., priority effects; **Fukami 2015**) and

391   velocity (e.g., **Evans et al. 2020**) both matter for community response to perturbation. Furthermore,

392   even an unsuccessful invasion by a single species that interacts only briefly with the resident

393   community can induce an alternative stable state with distinct functioning (**Amor et al. 2020**).

394   Variation in dispersal processes could therefore drive compositional and functional changes to

395   varying extents (e.g., **Fukami 2015**), resulting in varying magnitudes of decomposition legacy.

396 For example, in a field transplant experiment with passive dispersal, **Hawkes et al. (2017)** did not

397 find apparent mitigation of historical rainfall legacy in soil respiration. Give this result, we

398 recognize that our exploration of dispersal mechanisms and intensities is incomplete; our study

399 was mainly aimed at revealing underlying mechanisms and not meant to be exhaustive.
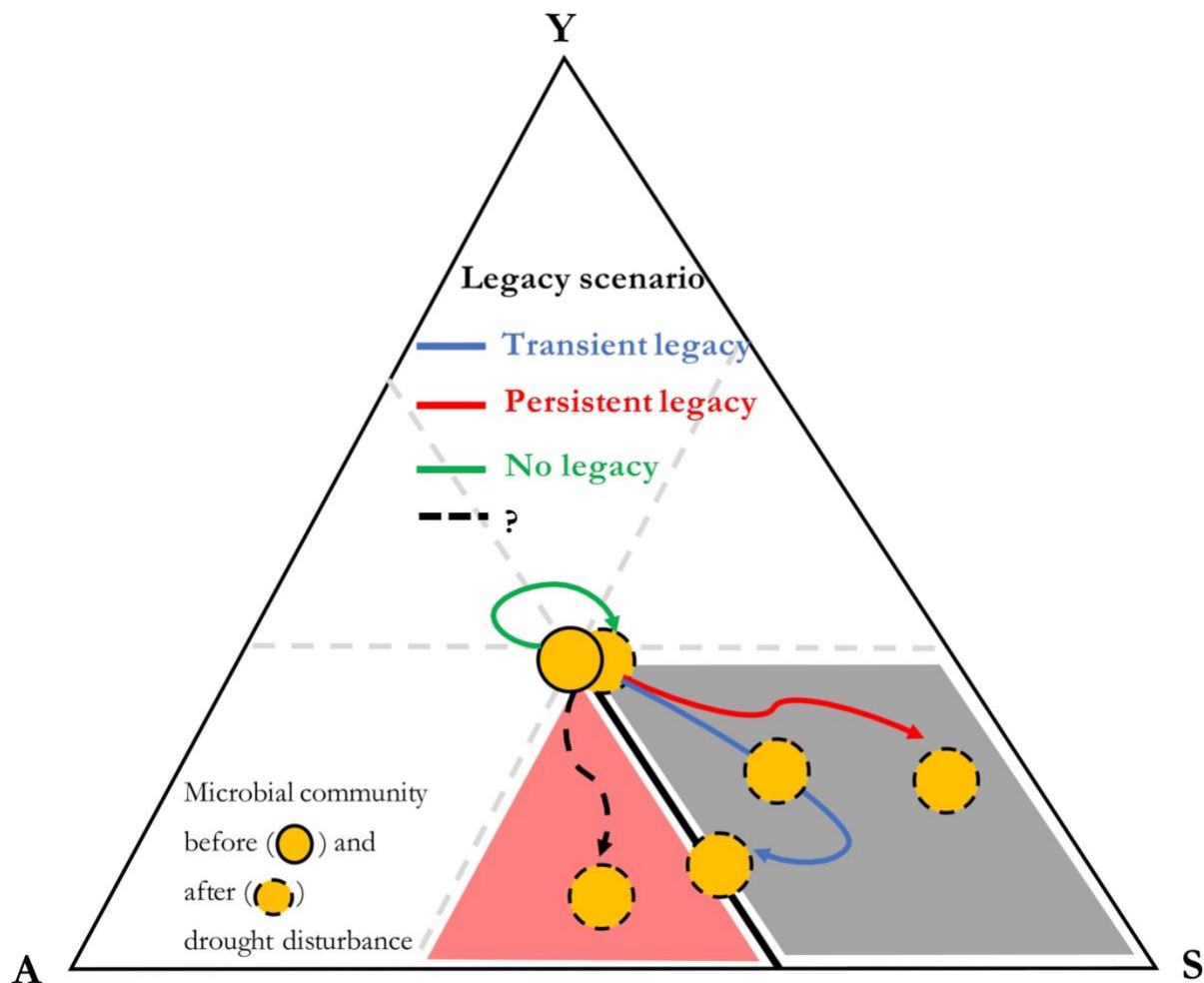

400

401 **Fig. 5 Overlay of drought legacy scenarios in YAS-constrained space.** Drought legacy is

402 contingent on the trajectory of a microbial community in the YAS space after drought disturbance.

403 There will be no legacy if a community does not move at all (green trajectory) or if it moves along

404 the thick black line. If an altered community remains in the grey region, a persistent legacy will

405 occur. However, if the community eventually leaves the grey region and returns to the thick black

406 line, a transient legacy can occur. We also propose that a community could move into the red

407 region with both increased drought tolerance and enzyme investment (but at the expense of growth

408 yield). Note: the positioning of the starting community in the center of the space (filled yellow

409 circle) is for illustration purposes only; real communities may start anywhere in the YAS space.

410

411 **A mechanistic conceptual framework**

412 We propose to organize legacy scenarios with based on the YAS framework, as illustrated

413 in **Fig. 5**. Drought legacies are ultimately determined by the trajectory of a community in a

414 conceptual space defined by enzyme investment, drought tolerance, and yield. Factors that affect

415 cellular metabolic tradeoffs between enzyme and osmolyte production may influence the

416 magnitude and/or duration of a drought legacy. For instance, when drought selects for a

417 community with higher drought tolerance but ultimately similar enzyme investment (e.g.,

418 moderate drought scenario; **Fig. 4A**), a transient legacy occurs. However, when more severe

419 drought selects for higher drought tolerance at the expense of enzyme investment (**Fig. 4A**), a

420 persistent legacy with impaired substrate decomposition can occur. In contrast, when the

421 community does not shift in strategy space (e.g., with dispersal present; **Fig. 4B**), even transient

422 legacies may not occur.

423 Tradeoffs in microbiomes and the biosphere more generally are often complex (e.g.,

424 **Berezovsky & Shakhnovich 2005; Ferenci 2016**). Some tradeoffs may be context-specific, and

425 even positive relationships between costly traits may be observed under certain conditions

426 (**Moreno-Gámez et al. 2020; Tikhonov et al. 2020**). These principles may apply to the

427 relationship between enzyme investment and drought tolerance which may depend on drought

428 intensity, dispersal, metabolic plasticity, and evolution history. For instance, a fourth legacy

429   scenario may exist with both increased osmolyte and enzyme investment that trade off against

430   lower yield (the red region in **Fig. 5**). Going forward, our study could be extended by broadening

431   the range of drought and dispersal scenarios and modifying the tradeoff assumptions in

432   DEMENTpy to gain a more complete picture of the mechanisms underlying drought legacies.

433

434   **Implications**

435   Our study revealed a tradeoff-mediated explanation for community-level trait changes that

436   lead to drought legacies in soil microbiomes. This mechanistic insight has consequences for

437   ecosystem responses to drought and other environmental changes. A more accurate quantification

438   of the magnitude and duration of drought legacies should enable better predictions of litter and soil

439   organic matter decomposition. Legacies of impaired decomposition, even when transient, may

440   enhance carbon sequestration in soil systems, but may also allow fuels to accumulate for the next

441   fire season, thereby increasing fire risk (e.g., **Pellegrini et al. 2018**). Additionally, impaired

442   decomposition can inhibit nutrient turnover and availability, thereby influencing plant productivity

443   and interactions with microbes (e.g., **Kaisermann et al. 2017**). These and other cascading changes

444   arising from microbiome legacies could initiate more complex ecosystem feedbacks. Evaluating

445   these implications requires a holistic approach that integrates physiological processes across

446   ecosystem to Earth system scales. Such an approach is crucial for predicting biogeochemical rates

447   in the context of projected global climate change that may induce legacy effects. Trait-based

448   models of both microbial and vegetation dynamics are proving essential in achieving this

449   predictive understanding.

450

451 **References**

452 Allison, S. D. (2012). A trait-based approach for modelling microbial litter decomposition.

453 Ecology letters, 15, 1058-1070.

454

455 Allison, S. D., & Goulden, M. L. (2017). Consequences of drought tolerance traits for microbial

456 decomposition in the DEMENT model. Soil Biology and Biochemistry, 107, 104-113.

457

458 Allison, S. D., Lu, Y., Weihe, C., Goulden, M. L., Martiny, A. C., Treseder, K. K., & Martiny, J.

459 B. (2013). Microbial abundance and composition influence litter decomposition response to

460 environmental change. Ecology, 94, 714-725.

461

462 Allison, S. D., & Martiny, J. B. (2008). Resistance, resilience, and redundancy in microbial

463 communities. Proceedings of the National Academy of Sciences, 105, 11512-11519.

464

465 Amor, D. R., Ratzke, C., & Gore, J. (2020). Transient invaders can induce shifts between

466 alternative stable states of microbial communities. Science Advances, 6, eaay8676.

467

468 Anderegg, W. R., Schwalm, C., Biondi, F., Camarero, J. J., Koch, G., Litvak, M., ... & Wolf, A.

469 (2015). Pervasive drought legacies in forest ecosystems and their implications for carbon cycle

470 models. Science, 349, 528-532.

471

472 Berdugo, M., Delgado-Baquerizo, M., Soliveres, S., Hernández-Clemente, R., Zhao, Y., Gaitán, J.

473 J., ... & Rillig, M. C. (2020). Global ecosystem thresholds driven by aridity. Science, 367, 787-

474 790.

475

476 Berezovsky, I. N., & Shakhnovich, E. I. (2005). Physics and evolution of thermophilic adaptation.

477 Proceedings of the National Academy of Sciences, 102, 12742-12747.

478

479 Birch, H. F. 1958. The effect of soil drying on humus decomposition and nitrogen availability.

480 Plant and Soil, 10, 9–31.

481

482 Borsa, A. A., Agnew, D. C., & Cayan, D. R. (2014). Ongoing drought-induced uplift in the western

483 United States. Science, 345, 1587-1590.

484

485 Conradi, T., Van Meerbeek, K., Ordonez, A., & Svenning, J. C. (2020). Biogeographic historical

486 legacies in the net primary productivity of Northern Hemisphere forests. Ecology Letters, 23, 800-

487 810.

488

489 Csonka, L. N. (1989). Physiological and genetic responses of bacteria to osmotic stress.

490 Microbiological Reviews, 53, 121-147.

491

492 Cuddington, K. (2011). Legacy Effects: The Persistent Impact of Ecological Interactions.

493 Biological Theory, 6, 203–210.

494

495 Evans, S.E., Wallenstein, M.D. (2012) Soil microbial community response to drying and rewetting

496 stress: does historical precipitation regime matter? Biogeochemistry, 109**,** 101–116.

497

498 Evans, S. E., & Wallenstein, M. D. (2014). Climate change alters ecological strategies of soil

499 bacteria. Ecology letters, 17, 155-164.

500

501 Evans, S. E., Bell-Dereske, L. P., Dougherty, K. M., & Kittredge, H. A. (2020). Dispersal alters

502 soil microbial community response to drought. Environmental Microbiology, 22, 905-916.

503

504 Falkowski, P. G., Fenchel, T., & Delong, E. F. (2008). The microbial engines that drive Earth's

505 biogeochemical cycles. Science, 320, 1034-1039.

506

507 Ferenci, T. (2016). Trade-off mechanisms shaping the diversity of bacteria. Trends in

508 Microbiology, 24, 209-223.

509

510 Fuchslueger, L., Bahn, M., Hasibeder, R., Kienzl, S., Fritz, K., Schmitt, M., ... & Richter, A. (2016).

511 Drought history affects grassland plant and microbial carbon turnover during and after a

512 subsequent drought event. Journal of Ecology, 104, 1453-1465.

513

514 Fukami, T. (2015). Historical contingency in community assembly: integrating niches, species

515 pools, and priority effects. Annual Review of Ecology, Evolution, and Systematics, 46, 1-23.

516

517   Glassman, S. I., Weihe, C., Li, J., Albright, M. B., Looby, C. I., Martiny, A. C., ... & Martiny, J.

518   B. (2018). Decomposition responses to climate depend on microbial community composition.

519   Proceedings of the National Academy of Sciences, 115, 11994-11999.

520

521   Green, J.K., Seneviratne, S.I., Berg, A.M. *et al.* (2019). Large influence of soil moisture on long-

522   term terrestrial carbon uptake. Nature, 565**,** 476–479.

523

524   Hawkes, C. V., & Keitt, T. H. (2015). Resilience vs. historical contingency in microbial responses

525   to environmental change. Ecology letters, 18, 612-625.

526

527   Hawkes, C. V., Waring, B. G., Rocca, J. D., & Kivlin, S. N. (2017). Historical climate controls

528   soil respiration responses to current soil moisture. Proceedings of the National Academy of

529   Sciences, 114, 6322-6327.

530

531   Herzschuh, U. (2020). Legacy of the Last Glacial on the present-day distribution of deciduous

532   versus evergreen boreal forests. Global Ecology and Biogeography, 29, 198-206

533

534   Hinojosa, M. B., Laudicina, V. A., Parra, A., Albert-Belda, E., & Moreno, J. M. (2019). Drought

535   and its legacy modulate the post-fire recovery of soil functionality and microbial community

536   structure in a Mediterranean shrubland. Global Change Biology, 25, 1409-1427.

537

538   Ives, A. R., & Carpenter, S. R. (2007). Stability and diversity of ecosystems. Science, 317, 58-62.

539

540 Kaisermann, A., de Vries, F. T., Griffiths, R. I., & Bardgett, R. D. (2017). Legacy effects of

541 drought on plant–soil feedbacks and plant–plant interactions. New Phytologist, 215, 1413-1424.

542

543 Karhu, K., Auffret, M., Dungait, J. *et al.* (2014) Temperature sensitivity of soil respiration rates

544 enhanced by microbial community response. Nature, 513, 81–84

545

546 Louca, S., Polz, M.F., Mazel, F. et al. (2018). Function and functional redundancy in microbial

547 systems. Nature Ecology Evolution, 2, 936–943.

548

549 Malik, A.A., Martiny, J.B.H., Brodie, E.L. *et al.* (2020). Defining trait-based microbial strategies

550 with consequences for soil carbon cycling under climate change. ISME J 14, 1–9.

551

552 Manzoni, S., Schimel, J. P., & Porporato, A. (2012). Responses of soil microbial communities to

553 water stress: results from a meta-analysis. Ecology, 93, 930-938.

554

555 Martiny, J., Martiny, A., Weihe, C. et al. (2017). Microbial legacies alter decomposition in

556 response to simulated global change. ISME J 11, 490–499.

557

558 McGill, B. J., Enquist, B. J., Weiher, E., & Westoby, M. (2006). Rebuilding community ecology

559 from functional traits. Trends in Ecology & Evolution, 21, 178-185.

560

561 Meisner, A., Rousk, J., & Bååth, E. (2015). Prolonged drought changes the bacterial growth

562 response to rewetting. Soil Biology and Biochemistry, 88, 314-322.

563

564 Moreno-Gámez, S., Kiviet, D. J., Vulin, C., Schlegel, S., Schlegel, K., van Doorn, G. S., &

565 Ackermann, M. (2020). Wide lag time distributions break a trade-off between reproduction and

566 survival in bacteria. Proceedings of the National Academy of Sciences, 117, 18729-18736.

567

568 Pellegrini, A., Ahlström, A., Hobbie, S. *et al.* (2018). Fire frequency drives decadal changes in soil

569 carbon and nitrogen and ecosystem productivity. Nature, 553, 194–198.

570

571 Potts, M. (1994). Desiccation tolerance of prokaryotes. Microbiological Reviews, 58, 755-805.

572

573 Rousk, J., Smith, A. R., & Jones, D. L. (2013). Investigating the long-term legacy of drought and

574 warming on the soil microbial community across five European shrubland ecosystems. Global

575 Change Biology, 19, 3872-3884.

576

577 Scheffer, M., Carpenter, S., Foley, J. A., Folke, C., & Walker, B. (2001). Catastrophic shifts in

578 ecosystems. Nature, 413, 591-596.

579

580 Schimel, J., Balser, T. C., & Wallenstein, M. (2007). Microbial stress-response physiology and its

581 implications for ecosystem function. Ecology, 88, 1386-1394.

582

583 Staver, A. C., Archibald, S., & Levin, S. A. (2011). The global extent and determinants of savanna

584 and forest as alternative biome states. Science, 334, 230-232.

585

586   Tikhonov, M., Kachru, S., & Fisher, D. S. (2020). A model for the interplay between plastic

587   tradeoffs and evolution in changing environments. Proceedings of the National Academy of

588   Sciences, 117, 8934-8940.

589

590   Tropini, C., Moss, E. L., Merrill, B. D., Ng, K. M., Higginbottom, S. K., Casavant, E. P., ... &

591   Bhatt, A. S. (2018). Transient osmotic perturbation causes long-term alteration to the gut

592   microbiota. Cell, 173, 1742-1754.

593

594   Wang, B., & Allison, S. D. (2019). Emergent properties of organic matter decomposition by soil

595   enzymes. Soil Biology and Biochemistry, 136, 107522.

596

597   Waring, B., Hawkes, C. V. (2018). Ecological mechanisms underlying soil bacterial responses to

598   rainfall along a steep natural precipitation gradient, FEMS Microbiology Ecology, 94, fiy001.

599

600   Vila, J. C., Jones, M. L., Patel, M., Bell, T., & Rosindell, J. (2019). Uncovering the rules of

601   microbial community invasions. Nature Ecology & Evolution, 3, 1162-1171.

602

603   Wieder, W. R., Allison, S. D., Davidson, E. A., Georgiou, K., Hararuk, O., He, Y., ... & Todd-

604   Brown, K., 2015. Explicitly representing soil microbial processes in Earth system models. Global

605   Biogeochemical Cycles, 29, 1782-1800.

606

1   Supporting Information

2   **Drought Legacies Mediated by Trait Tradeoffs in Soil Microbiomes**

3   Bin Wang [1], Steven D. Allison [1,2]

4   [1] Department of Ecology and Evolutionary Biology, University of California, Irvine, CA

5   [2] Department of Earth System Science, University of California, Irvine, CA

6

1 DEMENTpy

8   DEMENTpy is a trait-based modelling framework with spatially-explicit representation of

9   individual populations in microbial communities. The model version reported here updates the

10   physiological mechanisms (see **Supporting Fig. 1** for conceptual structure) and programming

11   approach (see **Supporting Fig. 7** for programming structure) to the DEMENT model that was

12   initially developed in 2012 (**Allison 2012**). The source code in Python is accessible at

13   https://github.com/bioatmosphere/DEMENTpy. Processes simulated in DEMENTpy are

14   described below.

1.1 Microbial community initialization

16   Using a trait-based approach, DEMENTpy initiates a microbial pool with a large number

17   of hypothetical taxa by randomly drawing values from distributions of physiological traits

18   (**Supporting Table 1**) and assigning them to different taxa. These hypothetical taxa in the

19   microbial pool with differing combinations of trait values are randomly placed on the spatial grid

20   to form a spatially structured microbial community. Illustrative animations are available at

21   https://bioatmosphere.github.io/DEMENTpy/, and see **Wang and Allison (2019)** for an

22   application of model spatial resolution for scaling up enzymatic heterogeneity. Trait distributions

23   are all assumed to follow uniform distributions, except that for simplicity, some trait values are

24   assumed to be constant, and values of some traits are derived from established correlations with

25   other traits. These distributions and assumptions are largely informed by field- and lab-based

26   empirical studies (**Allison 2012; Allison and Goulden 2017**).

27   The key traits determining mass balance in drought simulations are constitutive and

28   inducible rates of enzyme and osmolyte production. The richness of genes encoding different

29   enzymes and osmolytes is determined randomly for each taxon during model initialization.

30   Therefore, gene richness and production rate together determine the amounts of enzyme and

31   osmolyte a cell can produce. The rate of inducible osmolyte production is then normalized to a

32   value from 0 to 1, which is regarded as drought tolerance. This parameterization of drought

33   tolerance is an update to the previous DEMENT version which instead directly introduced a

34   drought tolerance parameter and imposed a penalty on carbon use efficiency accordingly (**Allison**

35   **and Goulden 2017**). Linking osmolyte production directly to drought tolerance is intended to be

36   more biologically realistic (**Schimel 2007**). Additionally, kinetic traits including Vmax and Km

37   are assigned to explicitly parameterize a certain number of different enzymes and transporters in

38   the model system.

39   **1.2 Metabolic production of enzyme and osmolyte**

40   Different individuals (hypothetical taxa) comprising the microbial community undergo

41   demographic processes of growth, mortality, and reproduction while degrading substrates and

42   assimilating monomers at rates dependent on temperature and water potential. From these

43   underlying processes emerge dynamics and functioning at both the microbial cell level and the

44   whole system level.

45   Substrate degradation rates are calculated based on the activities of enzymes with different

46   kinetic properties. Every enzyme degrades at least one substrate, and every substrate is degraded

47   by at least one enzyme. Monomer uptake is calculated based on transporter abundance and kinetic

48   traits which are specific to each taxon. The governing equation for both substrate degradation and

49   monomer uptake follows the Michaelis-Menten equation, which is constrained by temperature

50   (accounting for temperature impacts on enzymatic kinetics) and water potential (accounting for

51   moisture constraints on enzymatic kinetics and diffusion; **Allison and Goulden 2017**):

52
$$V = \frac{V_{max}f(T)[S][E]}{K_m+[S]} f(\psi)$$

53
$$f(T) = e^{\left(-\frac{\varepsilon}{R}\left(\frac{1}{T}-\frac{1}{T_{ref}}\right)\right)}$$

54
$$f(\psi) = e^{k\psi}$$

55   where *E* and *S* are matrices containing enzyme and substrate concentrations, respectively, *Vmax*

56   represents the enzyme catalytic constant, *Km* denotes the concentration of *S* at which *V* is one half

57   *Vmax*, ε is enzymatic activation energy, *R* is universal gas constant, and *k* is a coefficient controlling

58   water potential sensitivity that differs between degradation and uptake.

59   Cellular metabolism balances carbon upon uptake from degraded substrates and carbon

60   loss through constitutive and inducible metabolite production (**Supporting Fig. 3**). After growth

61   respiration (constrained by a constant), assimilated carbon is directed to enzyme and osmolyte

62   production along with their associated maintenance respiration rates, all of which are treated

63   simultaneously in the model without prescribing an order. The carbon remaining after these

64   processes accumulates toward biomass. We assume the constitutive osmolyte production rate

65   (*Osmo_Con*) varies across taxa independent of water potential, accounting for microbial allocation

66   to maintain water potential balance across the cell wall (**Csonka 1989; Potts 1994**). In contrast,

67   taxon-specific inducible production of osmolytes (*Oind*) depends on water potential as follows:

68

69
$$O_{ind}(i) = \begin{cases} O_{ind}(i), & \psi \geq \psi_{th} \\ O_{ind}(i)\,(1 - \alpha\psi), & \psi < \psi_{th} \end{cases}$$

70

71   where O_{ind}, is the i_{th} taxon's inducible osmolyte production rate, ψ is the daily water potential, α

72   is a coefficient determining water potential sensitivity, and ψ_{th} is a system water potential constant,

73   below which inducible osmolyte production is activated. Osmolyte stoichiometry is assumed to be

74   constant at C/N = 3, which governs consumption of N in intracellular metabolism. This ratio is

75   based on an average of the three most common osmotic compounds in bacteria (**Csonka 1989;**

76   **Potts 1994**): proline ($C_5H_9NO_2$), glycine betaine ($C_5H_{11}NO_2$), and glutamine ($C_5H_{10}N_2O_3$).

77   Mortality of microbial cells is simulated both deterministically by accounting for mass

78   balance relative to a threshold, and stochastically based on a death probability constrained by

79   drought tolerance and water potential. Here the taxon-specific mortality probability (*Mort*) is

80   calculated as:

81

82    $$Mort_i = Death\_basal_i[1 - Death\_rate_i(1 - Tol_i)(\psi - \psi_{th})\,]$$

83

84   where *Death_basal* is the i_{th} taxon's basal mortality probability, *Death_rate* is a death probability

85   coefficient controlling water potential sensitivity, *Tol* is the i_{th} taxon's drought tolerance, and ψ_{th}

86   is a system water potential constant. Microbial cells that fall below the biomass threshold or that

87   die randomly are removed from the microbial community and added into the substrate pools as

88   dead microbes. Microbial reproduction is calculated by splitting microbes into two equal halves,

89   followed by local dispersal to surrounding grid boxes on the spatial grid (**Allison 2012**).

90

91 **2. Calculation of community-level traits**

92 Community-level enzyme investment (E_{com}) and drought tolerance (D_{com}) weighted by

93 biomass are calculated as:

$$94 \qquad E_{com} = \sum_{i}^{n} E_i M_i$$

$$95 \qquad D_{com} = \sum_{i}^{n} D_i M_i$$

96

97 respectively, where E_i and D_i refer to the i_{th} taxon's enzyme production rate and drought tolerance,

98 respectively, and M_i is the relative biomass of the i_{th} taxon in the community.

99

100 **References**

101 Allison, S. D. (2012). A trait-based approach for modelling microbial litter decomposition.

102 Ecology letters, 15, 1058-1070.

103

104 Allison, S. D., & Goulden, M. L. (2017). Consequences of drought tolerance traits for microbial

105 decomposition in the DEMENT model. Soil Biology and Biochemistry, 107, 104-113.

106

107 Bugmann, H., Fischlin, A., & Kienast, F. (1996). Model convergence and state variable update in

108 forest gap models. Ecological Modelling, 89, 197-208.

109

110 Csonka, L. N. (1989). Physiological and genetic responses of bacteria to osmotic stress.

111 Microbiological Reviews, 53, 121-147.

112

113   Potts, M. (1994). Desiccation tolerance of prokaryotes. Microbiological Reviews, 58, 755-805.

114

115   Schimel, J., Balser, T. C., & Wallenstein, M. (2007). Microbial stress-response physiology and its

116   implications for ecosystem function. Ecology, 88, 1386-1394.

117

118   Wang, B., & Allison, S. D. (2019). Emergent properties of organic matter decomposition by soil

119   enzymes. Soil Biology and Biochemistry, 136, 107522.

Supporting Table 1 Microbial and enzyme parameters and their values

Parameter	Value	Unit	Note
max_size_b	2	mg cm-3	C quota threshold for bacterial cell division
Cfrac_b	0.825	mg mg-1	Bacterial C fraction
Nfrac_b	0.16	mg mg-1	Bacterial N fraction
Pfrac_b	0.015	mg mg-1	Bacterial P fraction
Crange	0.09	mg mg-1	Tolerance on C fraction
Nrange	0.04	mg mg-1	Tolerance on N fraction
Prange	0.005	mg mg-1	Tolerance on P fraction
C_min	0.086	mg cm-3	threshold C concentration for cell death
N_min	0.012	mg cm-3	threshold P concentration for cell death
P_min	0.002	mg cm-3	threshold C concentration for cell death
Uptake_C_cost_min	0.01	transporter mg-1 biomass C	Minimun per enzyme C cost as a fraction of uptake
Uptake_C_cost_max	0.1	transporter mg-1 biomass C	Maximum per enzyme C cost as a fraction of uptake
Uptake_Maint_cost	0.01	mg C transporter-1 day-1	Respiration cost of uptake transporters
Enz_per_taxon_min	0		Minimum number of enzymes a taxon can produce
Enz_per_taxon_max	40		Maximum number of enzymes a taxon can produce
Enz_Prod_min	0.00001	mg C mg-1 day-1	Minimum per enzyme production cost as a fraction of C uptake rate
Enz_Prod_max	0.0001	mg C mg-1 day-1	Maximum per enzyme producton cost as a fraction of C uptakte rate
Constit_Prod_min	0.00001	mg C mg-1 day-1	Minimum per enzyme production cost as a fraction of biomass C
Constit_Prod_max	0.0001	mg C mg-1 day-1	Maximum per enzyme production cost as a fraction of biomass C
Osmo_per_taxon_min	1		Minimum number of osmolyte a taxon can produce
Osmo_per_taxon_max	1		Maximum number of osmolyte a taxon can produce
Osmo_Consti_Prod_min	0.0000001	mg C mg-1 day-1	Minimum per osmolyte production cost as a fraction of biomass C
Osmo_Consti_Prod_max	0.000001	mg C mg-1 day-1	Maximum per osmolyte production cost as a fraction of biomass C
Osmo_Induci_Prod_min	0.01	mg C mg-1 day-1	Minimum per osmolyte production cost as a fraction of C uptake rate
Osmo_Induci_Prod_max	0.1	mg C mg-1 day-1	Maximum per osmolyte production cost as a fraction of C uptake rate
CUE_ref	0.5	mg mg-1	Growth efficiency at the reference temperature
CUE_temp	-0.005	mg mg-1	Growth efficiency change with enzyme investment
death_rate_bac	0.001		Bacterial death rate
basal_bac	10		Bacterial basal death probability
wp_th	-2.00	MPa	Water potential threshold at which osmolyte is induced
alpha	0.01	mg C mg-1 day-1	Osmolyte production change with water potential
Vmax0_min	5	mg substrate mg-1 enzyme day-1	Minimum Vmax for enzyme
Vmax0_max	50	mg substrate mg-1 enzyme day-1	Maximum Vmax for enzyme

Uptake_Vmax0_min	1	mg substrate mg-1 substrate day-1	Minimum uptake Vmax
Uptake_Vmax0_max	10	mg substrate mg-1 substrate day-1	Maximum uptake Vmax
Uptake_Ea_min	35	kj mol-1	Minimum activation energy for uptake
Uptake_Ea_max	35	kj mol-1	Maximum activation energy for uptake
Km_min	0.01	mg cm-3	Minimum Km
Uptake_Km_min	0.001	mg cm-3	Minimum uptake Km
Vmax_Km	1	mg enzyme day cm-3	Slope for Km-Vmax relationship
Vmax_Km_int	0	mg cm-3	Intercept for Km-Vmax relationship
Uptake_Vmax_Km	0.2	mg biomass day cm-3	Slope for uptake Km-Vmax relationship
Uptake_Vmax_Km_int	0	mg cm-3	Intercept for uptake Km-Vmax relationship
Specif_factor	1		Enzyme efficiency-specificity

120

Supporting Table 2 Substrate concentrations initialized in DEMENT simulations (mg cm^{-3}).

Substrate	C	N	P
DeadMic	0	0	0
DeadEnz	0	0	0
Cellulose	146.89	0	0
Hemicellulose	85.855	0	0
Starch	12.21	0	0
Chitin	4.9952	0.83254	0
Lignin	48.51	0.40425	0
Protein1	10.6	2.09704	0
Protein2	10.6	2.09704	0
Protein3	10.6	2.09704	0
OrgP1	12.48	0	0.478469
OrgP2	1.8182	0.79745	0.478469

121
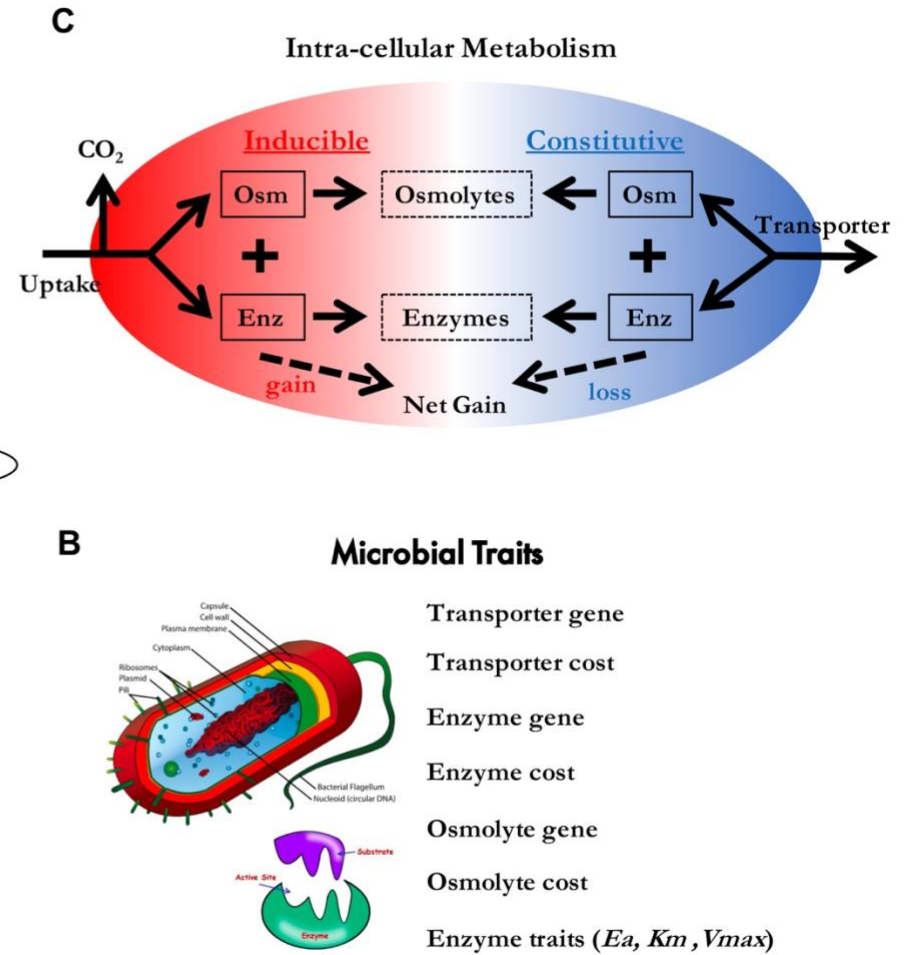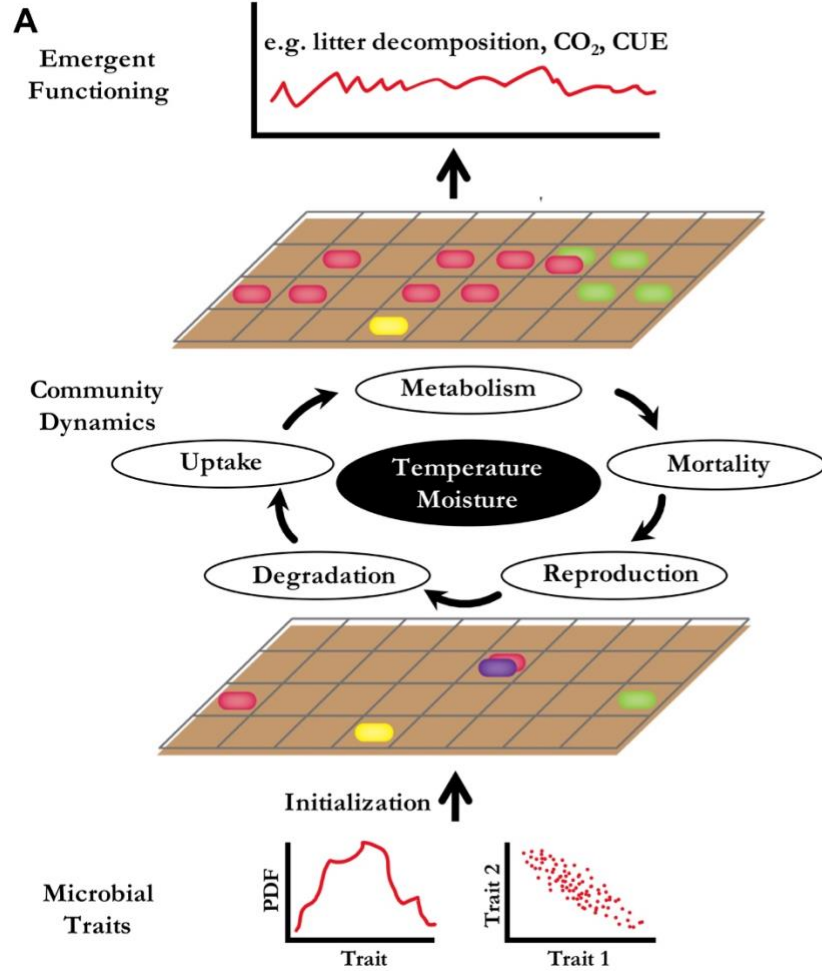
122

123   **Supporting Fig. 1 DEMENTpy conceptual structure (A), microbial traits (B), and intra-cellular metabolism (C).**

124
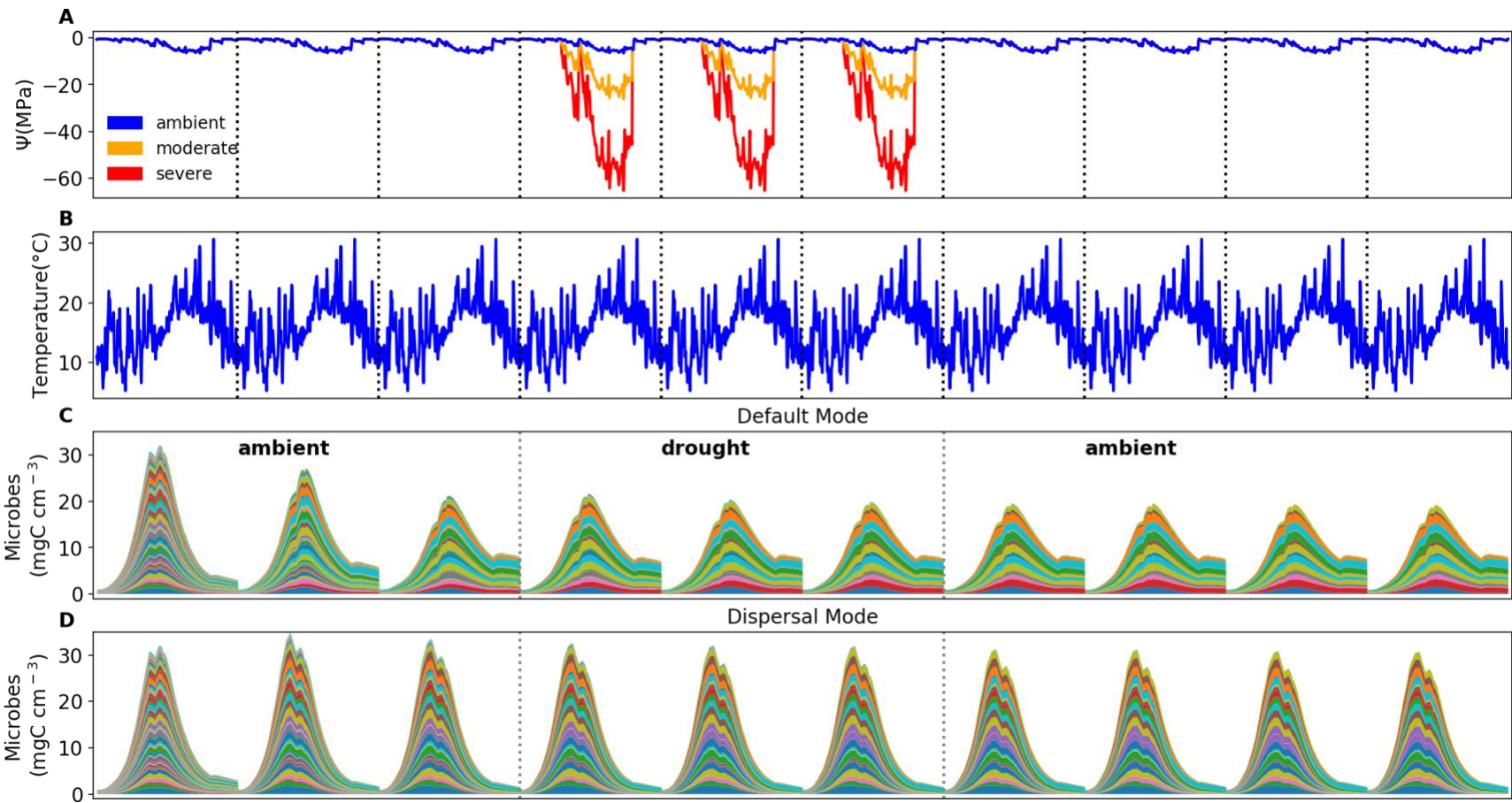
Supporting Fig. 2 Environmental forcing and microbial community dynamics. (**A**) Ambient daily water potential for 2011, with
the orange and red lines denoting the moderate and severe drought scenarios, respectively. Drought forcing was obtained by multiplying
the ambient water potential across the dry season (from April through September) by 4 and 10, respectively. (**B**) The corresponding
daily temperature in 2011. (**C, D**) Microbial community dynamics of the default vs. dispersal mode over 10 years under the ambient

129   scenario. The simulation comprises three phases as separated by the dashed grey lines: a spin-up phase of three years to realize a

130   relatively stable community; a disturbance phase imposing different drought scenarios for three years; and a final recovery phase after

131   drought disturbance for four years. Colored bands represent biomasses of hypothetical taxa.

132
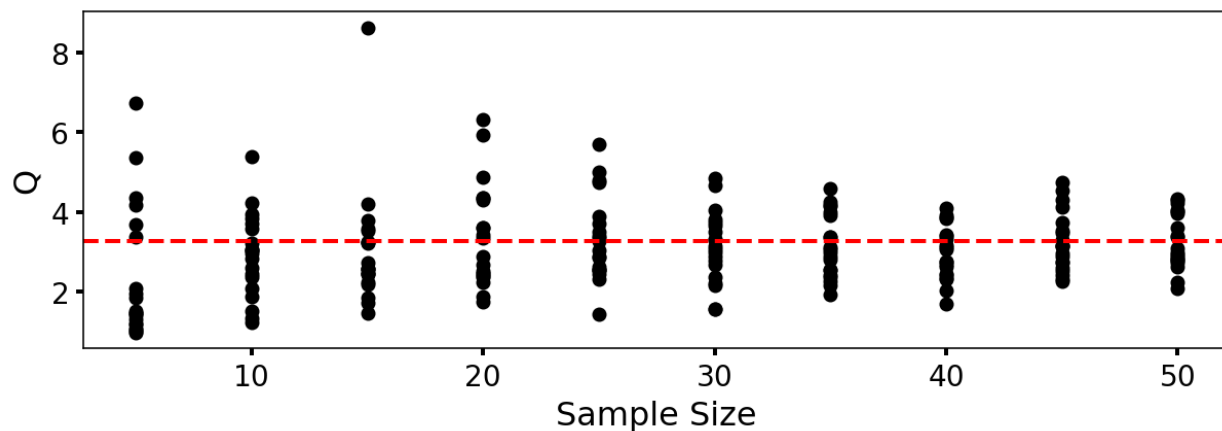
Supporting Fig. 3 DEMENTpy (v1.0) stochasticity convergence analysis. Q (quotient) is
calculated as (90% percentile -10% percentile)/median substrate degradation following Bugmann
et al. (1996). Each sample size has 20 replicates that were randomly drawn from a sample pool of
112 runs. This analysis illustrates that a sample size (i.e., ensemble of simulations) of 40 displays
relatively stable, convergent variation and that balances the tradeoff between precision and.
consumption of computing resources.
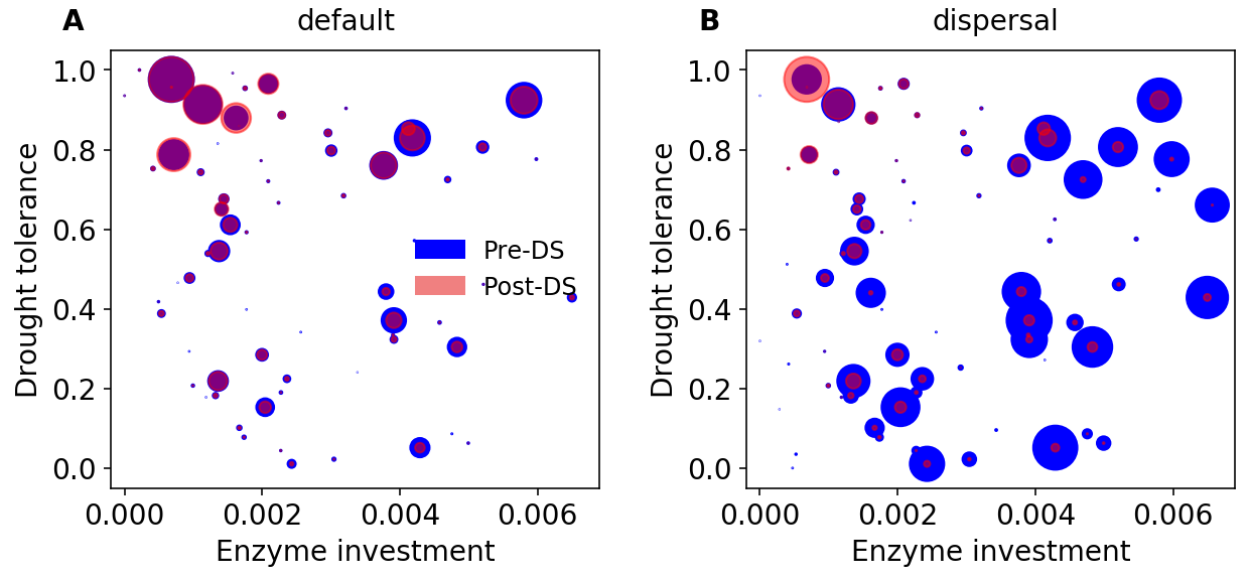
Supporting Fig. 4 Taxonomic changes in traits across the dry season. (A) Taxon-specific traits of drought tolerance and enzyme investment of a microbial community without dispersal before (blue) and after the dry season (red) under the ambient scenario. (**B**) The same for a microbial community with dispersal. Each point corresponds to a different taxon, and the size is proportional to its biomass.

145
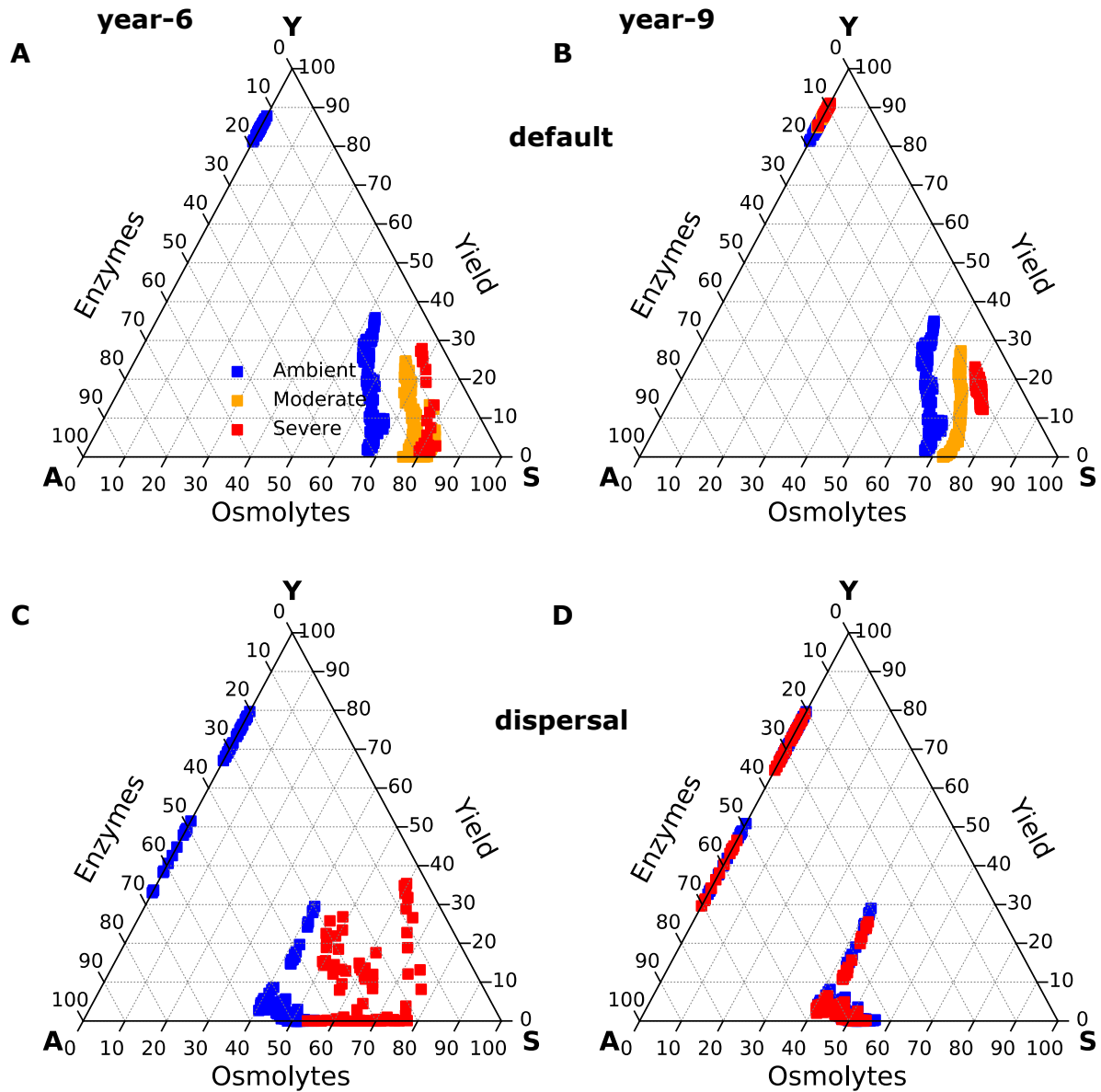
Supporting Fig. 5 Ternary plots of community-level allocation of assimilated carbon among enzymes, osmolytes, and yield over time under different drought scenarios. (A, B) Enzyme-Osmolyte-Yield tradeoff of communities during year 6 (3rd year under drought) and year 9 (3rd year after drought), respectively, of the default mode (without dispersal). (**C, D**) The same for the dispersal mode. The Y (Yield), A (Acquisition), and S (Stress tolerance) labels at the vertices

151   correspond to yield, enzymes, and osmolytes, respectively. Points with negative net biomass gain

152   were omitted.

153

154
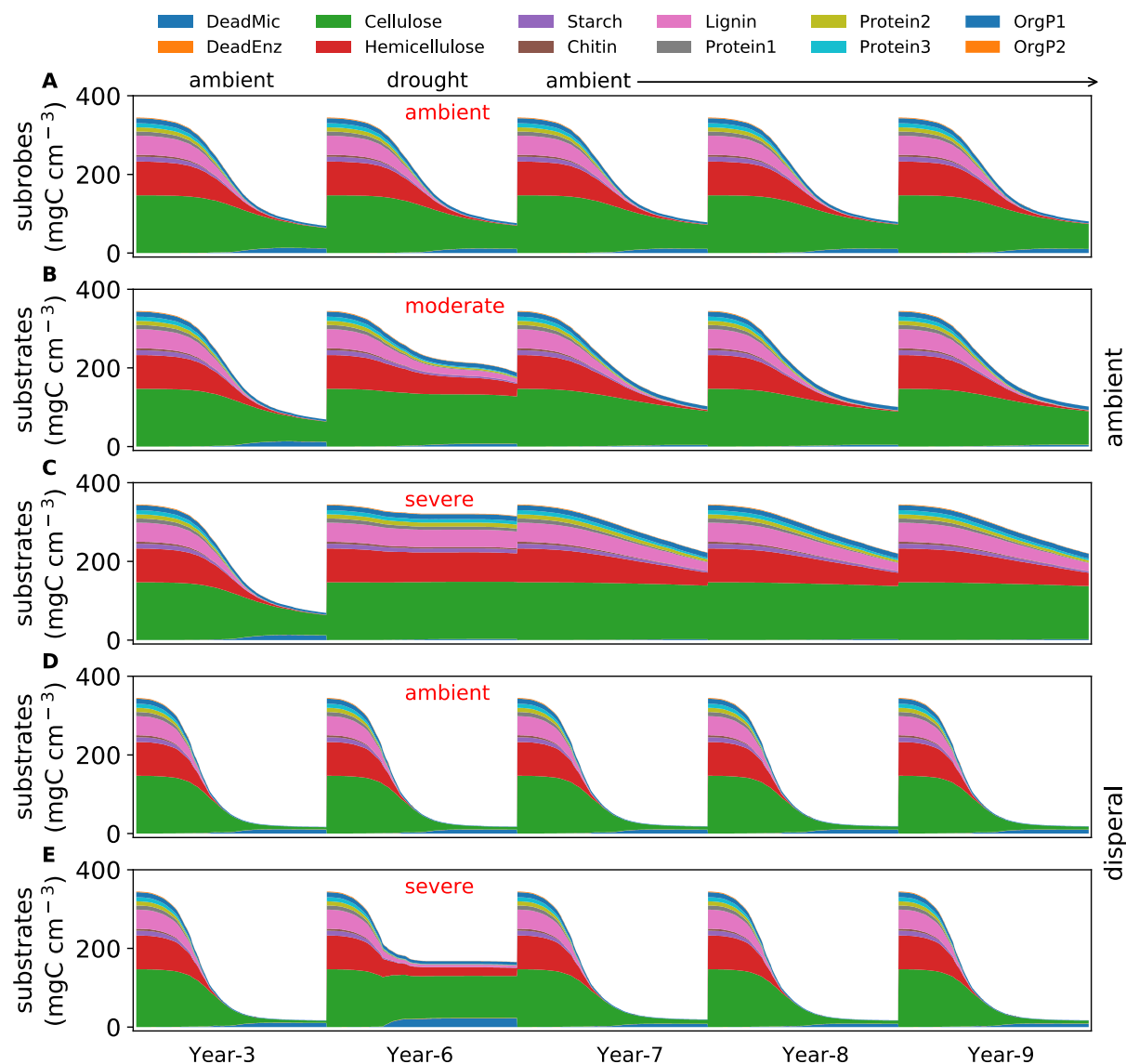
Supporting Fig. 6 Substrate-specific dynamics under differing drought scenarios. (A, B, C)

Dynamics under ambient, moderate, and severe drought scenarios in default mode for year 3 and

year 6 (the 3rd year under drought disturbance) through year 9. (**D, E**) The same for the dispersal

mode but with only ambient and severe scenarios. Each color band represents one type of 12

different substrates.

DEMENTpy Programming Structure
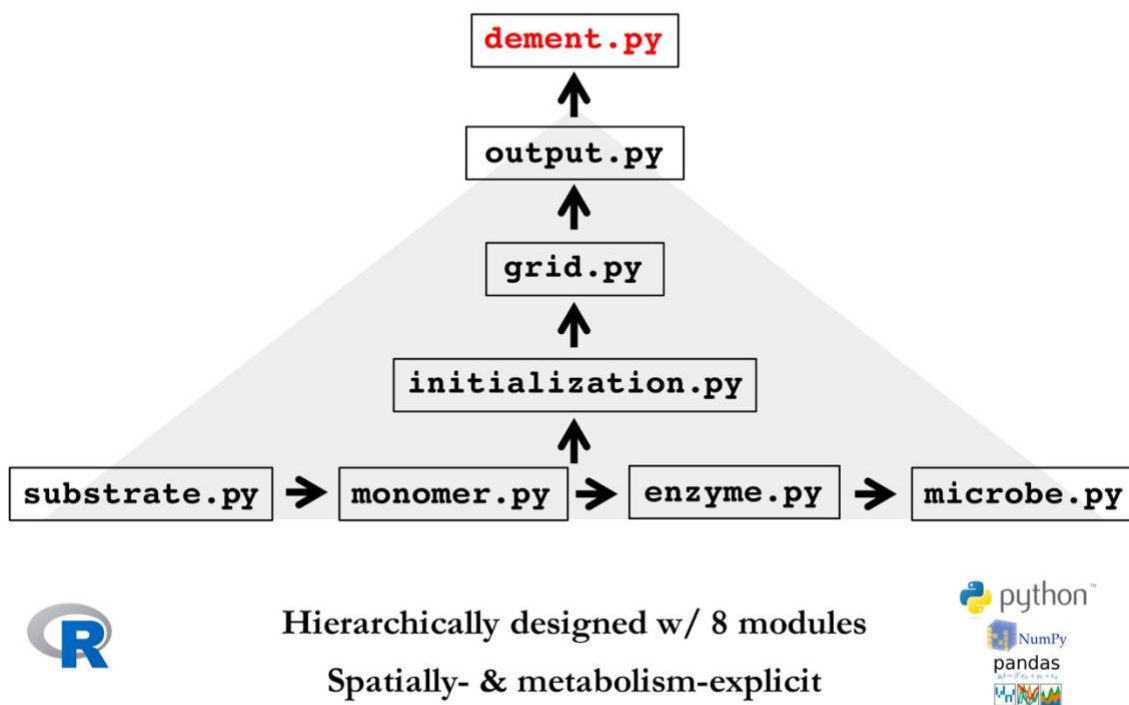
Supporting Fig. 7 DEMENTpy programming structure. DEMENTpy emerges from hierarchically restructuring and mechanistically updating DEMENT, which was programmed in R.